Evaluation of the Energy-Efficiency of an Aerated Slurry-Infiltrated Mesh Building System with Biomass-Based Insulation

Areej T. Almalkawi[a,*], Parviz Soroushian[b], Som S. Shrestha[c]

[a] Dept. of Civil and Environmental Engineering, Michigan State University, 3546, Engineering Building, E. Lansing, MI, United States

[b] Metna Corporation, 1926, Turner Street, Lansing, MI, United States

[c] Building Technologies Research and Integration Center, Oak Ridge National Laboratory, Oak Ridge, TN, 37831-6070, United States

[*] E-mail: almalkaw@msu.edu, atmalkawi05@eng.just.edu.jo (A.T. Almalkawi)

Experimental investigations and numerical analyses were conducted on the thermal attributes of a building system made with locally available structural and insulation materials. The structural material, which also offers some insulation qualities, is referred to as aerated slurry-infiltrated mesh. The insulation materials used in this building are based on biomass; the alternatives considered here include ground wood, shredded straw, and cellulose. Thermal conductivity tests were performed on aerated slurries of different bulk densities, and on the biomass-based insulation materials, some of which were prepared with different bulk densities. The competitive merits of the biomass-based indigenous insulation materials were assessed. The correlations between bulk density and thermal conductivity were evaluated and rationalized based on the prevalent mechanisms of heat transfer in different materials. The effects of temperature on the thermal conductivity of different biomass-based indigenous insulation materials were investigated. For wall insulation, a cost analysis was conducted in order to select the optimum insulation level. The thermal mass of the aerated slurry-infiltrated mesh building system was found to favor its energy-efficiency when compared with a similar wood building.

This manuscript has been co-authored by UT-Battelle, LLC, under contract DE-AC05-00OR22725 with the US Department of Energy (DOE). The US government retains and the publisher, by accepting the article for publication, acknowledges that the US government retains a nonexclusive, paid-up, irrevocable, worldwide license to publish or reproduce the published form of this manuscript, or allow others to do so, for US government purposes. DOE will provide public access to these results of federally sponsored research in accordance with the DOE Public Access Plan (http://energy.gov/downloads/doe-public-access-plan).

1. Introduction

Beneficial use of thermal mass is an important consideration in design of climate-adapting sustainable buildings [1-3]. The growing need for energy-efficient buildings with optimum thermal comfort has increased the reliance on thermal mass to meet these requirements [4,5]. Construction of buildings with heavier materials, including concrete and masonry, used within the insulation system, leads to reduced temperature swing in the indoor temperature [6]. The high thermal inertia of such buildings allows for effective radiant heating in winter, and reduces the chance of indoor overheating in summer [7-9]. Building systems with high thermal mass, on the other hand, require more time to cool down or heat up. This feature could translate into thermal discomfort; more energy could also be used for heating and cooling to compensate for this effect [10]. There are thus conditions where buildings constructed with lighter materials (e.g., wood) can offer improved thermal performance when compared with heavier buildings [7,11]. Opting for an effective amount of thermal mass is always critical, and depends on a number of factors, including climatic conditions, occupancy patterns, internal heat gains, building orientation, and types of mechanical devices [12,13]. These factors should be considered integrally with the thermal mass and insulation requirements to minimize the overall energy demand and maximize the thermal comfort of the building interior [11,14]. The availability of new building materials offer more options to address this challenging issue. Examples include hollow block walls, ventilated slabs [15], phase change materials (PCM) [16], dynamic insulation systems [17], and ultra-light-weight concrete (ULWC) [18].

The investigation reported herein covers the thermal aspects of developing a new building material, referred to as aerated slurry-infiltrated mesh, which is focused on maximum use of locally available materials (including insulation materials) towards development of sustainable, structurally safe and energy-efficient buildings [39,41]. The matrix developed here is an aerated slurry that also offers desired rheological attributes for infiltrating fabric and mesh reinforcement systems [40,42]. Aerated cementitious materials (e.g., aerated concrete) have been developed mostly to provide thermal insulation qualities [35-38]. This building system offers an intermediate thermal mass, which occurs between those of wood and concrete building systems. The thermal mass provided is selected primarily based on structural requirements, and should be supplemented with proper indigenous insulation levels for realizing desired energy-efficiency

and thermal comfort [19]. The selection of thermal insulation must satisfy many criteria, including energy performance, economics, environmental impacts, and compatibility with structural design.

This work covers measurement of the insulation qualities of aerated slurry-infiltrated mesh and biomass-based insulation materials. A model building system made with aerated slurry-infiltrated mesh structural system was subjected to thermal analysis in order to identify the wall, roof and floor insulation requirements to meet both loading and heating demand for the building. Desired levels of thermal insulation were identified. The results are used, together with the structurally governed mass of the building, to identify the insulation conditions that yield desired thermal performance. A comparative analysis was conducted between the energy demands of building systems made with aerated slurry-infiltrated mesh versus wood.

2. Experimental evaluation of insulation qualities

2.1. Materials

2.1.1. Aerated slurry

The aerated slurry had a water/cement ratio of 0.6; a foaming agent was used at different dosages to produce hardened material bulk densities ranging from 0.65 to 1.15 g/cm^3 (in oven-dried condition). The aerated slurry was prepared by first mixing a foaming agent (saponin) with the mixing water for 6 min, using a drill with a blade attached to it and operated at a rotational speed of 1200 rpm (Fig. 1a). The resulting foamed mixing water was then added to cement and mixed for 12 min in a planetary mortar mixer (Fig. 1b) to produce a homogeneous aerated slurry.

The thermal conductivity test specimens (Fig. 2.) were in the form of thin circular plates. They were molded and consolidated under external vibration, demolded after 24 h of storage in sealed condition, and then cured at >95% relative humidity) and room temperature to reach 7 days of age. The specimens were then oven-dried for 24 h at 105±5°C, weighed for evaluating their bulk density, and subjected to the thermal conductivity experiment.

2.2. Biomass-based insulation materials

Three categories of biomass-based insulation were used in this investigation: (i) ground wood; (ii) shredded straw; and (iii) a commercially available blow-in cellulose insulation. These three insulation materials are described in the following. The thermal conductivity test specimens of different biomass based insulation materials had the same geometric attributes as the aerated slurry thermal conductivity test specimens. Wheat straw was shredded in the hammer mill shown in Fig. 3. This mill is Type MUR manufactured by the American Pulverizer Co.; it has a 10mm diameter sieve installed on it.

2.3. Thermal conductivity test method

Thermal conductivity measurements were made using a test setup (Fig. 4) manufactured by Holometrix GHP that meets the ASTM C177 requirements. In this test, two similar specimens are placed between a middle hot plate and two outside cold plates. The hot and cold plates were typically kept at constant 30°C and 20°C temperatures, respectively, to represent the outdoor and indoor temperatures. The effects of temperature on the thermal conductivity of different insulation materials was also investigated. Temperatures on the hot and cold plates as well as the heat flow were monitored over a 24-hour time period. The results, after the processed reached equilibrium, were used to calculate the thermal conductivity of test specimens.

The thermal conductivity test specimens used in this experimental work were circular plates of 195 mm diameter and 25.4 mm thickness. They were produced by containing the loose insulation materials within a ring fabricated using a flexible polypropylene sheet of 1 mm thickness (Fig. 5). The ground wood, shredded straw and commercially available cellulose insulation test specimens are shown in Fig. 6.

2.3.1. Thermal simulation and design of the building system

A simple aerated slurry-infiltrated chicken mesh building designed to meet structural requirements was subjected to thermal analysis in order to evaluate its insulation requirements. The building planar dimensions are 4.9 m × 9.8 m, and its height is 2.4 m. The building structure (Fig. 7) comprises nine aerated slurry-infiltrated chicken mesh frames of 0.75 g/cm^3 bulk density to which external wall, internal wall all, roof and ceiling aerated slurry-infiltrated chicken mesh sheets are screwed. The floor also comprises aerated slurry-infiltrated chicken mesh sheets,

which span the frame footings and are supported on compacted sand. All (roof, ceiling, wall and floor) sheets have a bulk density of 0.75 g/cm^3. The interior and exterior sheets are 19 and 25.4 mm thick, respectively.

2.3.2. Thermal simulation of the building system

The building system considered here (Fig. 8) serves military purposes, and is used for business and residential occupancy during the day and at night, respectively. The design factors used in simulation of the building system using the eQUEST software are introduced in Table 1. The eQUEST software allows for multiple simulations of alternative building designs for comparative estimation of energy cost [21-23]. The energy-efficiency of the building system made with aerated slurry-infiltrated chicken mesh should be compared with those fabricated with wood that is prevalent in construction of small buildings.

Based on the test data introduced earlier, the thermal properties of the aerated slurry and the biomass insulation used in thermal analysis of the building are presented in Table 2. This table also presents typical thermal properties of plywood that is used as the control material used in construction of the conventional alternative to the building system considered here.

The thermal analysis investigate the effects of the thermal insulation levels of walls, roof and floor on the energy use of the building. Comparative analyses were also performed on the new building system versus a conventional wooden alternative to this system.

3. Results and discussion

3.1. Ground wood insulation

Wood branches collected locally (in air-dried condition) were ground using a hammer mill. The ground wood was passed through a sieve with 2.36 mm opening. While the ground wood insulation was used without any treatment; mitigation of microbial degradation may require their treatment. Fig. 9 Shows the particle size distribution of the ground wood insulation. The median particle size was about 0.8 mm, with particles ranging in size from 0.3 to 0.5 mm. The loosely packed ground wood had a bulk density of 0.291 g/cm^3.

The length distribution of shredded straw is presented in Fig. 10. Most straw fibrils are noted to be less than 1.5 mm in length. The loosely packed shredded straw insulation provided a bulk density of 0.069 g/cm^3.

3.1.1. Commercially available cellulose

The commercially available cellulose (Green Fiber) insulation used in this investigation is available as a "low dust blow-in" insulation. According to the manufacturer, this insulation would provide a thermal conductivity of 0.042 W m^{-1} K^{-1} at 25°C when packed loosely with a bulk density of 0.056 g/cm^3. The cellulose insulation was used in this investigation at the manufacturer's recommended bulk density of 0.056 g/cm^3, and also in loosely and densely packed conditions with bulk densities of 0.068 and 0.034 g/cm^3, respectively.

3.1.2. Thermal conductivity test results

Fig. 11 Presents the measured values of thermal conductivity for the ground wood, shredded wheat strawand cellulose (0.056 g/cm^3 bulk density) insulation materials were 0.0516, 0.0379 and 0.0389 W/m.K, respectively. The indigenous insulation materials (ground wood and shredded straw) thus provide insulation qualities that are of the same order of magnitude of that provided by the commercially available cellulose insulation. The bulk density and thermal conductivity of shredded straw and cellulose were comparable. Ground wood with a higher bulk density provided a higher level of thermal conductivity.

As noted earlier, the cellulose insulation material was tested at different bulk densities. The thermal conductivity test results presented in Fig. 12. Indicate that changing the bulk density to less than or more than the manufacturer's recommended level both reduce the thermal conductivity of the cellulose insulation. The thermal conductivity of these loose insulation materials is governed by a combination of conduction, convection and radiation. Their thermal conductivity is influenced by a number of factors including porosity and pore size distribution [20].

The effects of temperature on the thermal conductivity of the biomass-based loose insulation materials were also investigated (Fig.13). In this series of tests, the temperature difference of hot and cold plates was kept constant at 10°C; the effects of the mean temperature (of hot and cold

plates) on thermal conductivity were investigated. Thermal conductivity is observed to increase with increasing temperature; this effect is less pronounced in the case of the ground wood insulation. Conductive, convective and radiative heat transfer are influenced differently by temperature (and temperature gradient). The trends in temperature effects on thermal conductivity depend, among other factors, on the pore size of insulation materials [20]. The observed rise in thermal conductivity with increasing temperature is not unusual for insulation materials with multi-faceted heat transport mechanisms.

The thermal conductivity test results for aerated slurries of different bulk densities are presented in Fig. 14. The pore system in aerated slurry comprises isolated individual pores. Convective heat transfer can thus occur only within pores (and not between them). Given this condition, and since the cementitious binder is thermally more conductive than air, replacement of air with the cementitious matrix in aerated slurries of higher densities would produce higher thermal conductivities.

3.1.3. Energy consumption

The building system comprises interior and exterior aerated slurry-infiltrated mesh walls, with biomass insulation placed in between the two sheets. Fig. 15 Shows the effects of the wall insulation (with roof and floor insulation kept constant) on the annual heating and cooling loads of the building. Beyond an R-value (US) of 20 wall insulation, increasing the insulation level does not reduce the heating and cooling loads of the building. Below this level of insulation, gains in the energy-efficiency of the building can be realized by adding to the wall insulation. The thickness of the biomass insulation with 0.039 W/mk thermal conductivity required to provide this level of wall insulation is 0.137 m (13.7 cm). Structural design requirements provide more than adequate spacing between exterior and interior wall sheets to place this level of biomass insulation.

The effects of roof insulation level on the annual heating and cooling loads of the building are presented in Fig. 16. The heating and cooling loads are observed to decrease with increasing roof insulation up to an R-value (US) of 10, beyond which the benefits of further increasing the roof insulation level are minimal. A biomass insulation thickness of 6.85 cm would provide this

required level of insulation. The cavity between the roof and ceiling sheets, decided based on structural requirements, is more than adequate for providing this level of insulation.

The floor of the building system comprises an aerated slurry-infiltrated chicken mesh supported on 20.3 cm of compacted sand which provides a thermal conductivity of about 0.3 W/mK. The effects of the floor insulation levels on the annual heating and cooling loads presented in Fig. 17. indicated that the heating and cooling energy consumption of the building decrease with increasing floor insulation up to about an R-value (US) of 4, beyond which the effects of further increasing the floor insulation level on the building energy use is minimal. Considering the insulation level provided by the aerated slurry-infiltrated chicken mesh sheet, 21 cm of compacted sand would be required under the floor sheets. Consideration of the insulation value of the aerated slurry-infiltrated chicken mesh floor sheets would reduce the required thickness of the compacted sand acting as insulation to 19 cm. The available compacted sand thickness of 20.3 cm is thus adequate for providing the required level of floor insulation.

3.1.4. Optimization of the wall insulation condition

Heat loss from the building that is subject of this investigation occurs largely via transfer of heat through exterior walls in winter, noting that these walls constitute the largest surface area of the building envelope [24,25]. An investigation was conducted to assess the optimum wall insulation condition, focusing on heat loss through walls [26,27] which minimizes the cost of meeting the energy demand of the building [28]. Fig. 18 Shows the effects of the wall insulation level on the energy use cost, the insulation cost, and the total cost. The total cost is observed to be minimized at wall insulation levels ranging from R-value (US) of 5−8, which correspond to biomass insulation thicknesses occurring within the 3.4−5.5 cm range.

3.1.5. Comparison with a conventional wood building

While the aerated slurry-infiltrated mesh building structure is developed to be lightweight, it still weighs more than a conventional building system with wood structure. The thermal mass of the aerated slurry-infiltrated mesh building would thus be larger than that of a wood building. A larger thermal mass generally reduces the energy demand of a building, and favorably influences thermal comfort [29]. Thermal time constant (TTC) is a thermal attribute of building envelopes

that incorporates thermal mass. TTC is defined as the heat stored in the whole envelope (including internal air) per unit of heat transmitted to or from the outside through the elements surrounding the enclosure and by ventilation [30,31]. It is the product of heat capacity (Q) and thermal resistance (R). TTC provides an indication for the effective thermal capacity of a building. A shorter value of TTC indicates that a smaller heat flux would be required to achieve a unit change in temperature. A longer TTC value, on the other hand, suggests that the high thermal inertial of the building suppresses indoor temperature fluctuations.

The value of heat capacity per unit area (Q_A, J/m^2. K) can be calculated as follows [32]:

$$Q_A = \rho.d.c_p$$

where, r is the material density (kg/m^3), d is the thickness of the material (m), and c_p is the specific heat of the material (J/kg.K). In calculating TTC_A (TTC per unit area, seconds) of a composite wall, the Q_A. R value of each layer, including the outside and inside air layers, is calculated in sequence:

$$TTC_A = \sum_{i=1}^{n} Q_{Ai} \cdot R_i$$

where, Q_{Ai}:$R_i = (\rho.d.c_p).(R_0 + R_1 + \ldots + R_i)$, and n is the number of layers.

The value of TTC for each surface is the product of TTC_A and the surface area. Surfaces of higher TTC value reflect further benefits that can be realized from thermal mass [33,34]. For the walls (Fig. 19) of the building system designed with aerate slurry-infiltrated mesh, the value of TTC_A was 13% larger than that designed with plywood (CDX). The total cooling and heating energy demands of the two building systems over a 12-month period are presented in Fig. 20 and Fig. 21., respectively. The aerated slurry-infiltrated mesh building is observed to be more energy-efficient than the wood building, which can be largely attributed to its larger thermal mass.

4. Conclusions

Experimental and numerical investigations were conducted towards development of a building system that can be constructed using locally available structural and insulation materials. The

structural material used here is referred to as aerated slurry-infiltrated mesh. The insulation materials are biomass-based, and include ground wood, shredded straw, and cellulose. The following conclusions were derived based on the experimental and numerical data generated in this work: (i) Shredded straw with lengths less than 1.5 mm and a bulk density of about 0.069 g/cm^3 in oven-dried condition as well as ground wood with a particle size distribution largely covering the 0.5−2.5 mm range and a bulk density of about 0.291 g/cm^3 provided viable levels of thermal conductivity which were comparable to those provided by commercially available cellulose insulation materials. (ii) Changing the bulk density of the loose biomass-based insulation materials to less than or more than a particular level reduces their thermal conductivity. The thermal conductivity of these loose insulation materials is governed by a combination of conduction, convection and radiation. A number of factors, including porosity and pore size distribution, influences their thermal conductivity. (iii) Thermal conductivity of loose biomass-based insulation materials included with increasing temperature; this effect was less pronounced in the case of the ground wood insulation. Conductive, convective and radiative heat transfer are influenced differently by temperature (and temperature gradient). The trends in temperature effects on thermal conductivity depend, among other factors, on the pore size of insulation materials. The observed rise in thermal conductivity with increasing temperature is not unusual for insulation materials with multi-faceted heat transfer mechanisms. (iv) In the case of aerated slurry, thermal conductivity was found to increase with increasing bulk density. The pore system in aerated slurry comprises isolated individual pores. Convective heat transfer can thus occur only within pores (and not between them). Given this condition, and since the cementitious binder is thermally more conductive than air, replacement of air with the cementitious matrix in aerated slurries of higher densities would produce higher thermal conductivities. (v) Thermal analysis of a building system made with aerated slurry-infiltrated mesh led to identification of wall, roof and floor insulation levels beyond which further rise in insulation level does not produce notable gains in energy efficiency. Thicknesses of typical biomass-based insulation (and compacted sand in the case of floors) for providing the identified levels of insulation were determined. The structural design provides adequate space for placement of the required biomass-based insulation. Optimum levels of wall insulation were identified based on cost considerations. (vi) The thermal mass of the aerated slurry-infiltrated mesh building system was

found to benefit its energy efficiency when compared with an equivalent building fabricated with wood.

Acknowledgments

The work reported herein was funded by the U.S. Army Grant No. W9132T-16C-0003 -USA.

References

[1] Y. Park, Adapting and Communicating Urban Climate by Design, 2015.

[2] E. Karol, Understanding possibilities: thermal comfort using climatic design with low energy supplementation, Eng. Build. 157 (15 December 2017) 30-34.

[3] Comparative study of the mechanical and thermal properties of lightweight cementitious composites, Construct. Build. Mater. 159 (20 January 2018) 316-328.

[4] M. Perino, V. Serra, Switching from static to adaptable and dynamic building envelopes: a paradigm shift for the energy efficiency in buildings, J. Façade Des. Eng. 3 (2) (2015) 143-163.

[5] F. Stazi, et al., The effect of high thermal insulation on high thermal mass: is the dynamic behaviour of traditional envelopes in Mediterranean climates still possible? Eng. Build. 88 (2015) 367-383.

[6] Thermal-resistant lightweight concrete with polyethylene beads as coarse aggregates, Construct. Build. Mater. 164 (10 March 2018) 739-749.

[7] H. Johra, P. Heiselberg, Influence of internal thermal mass on the indoor thermal dynamics and integration of phase change materials in furniture for building energy storage: a review, Renew. Sustain. Eng. Rev. 69 (2017) 19-32.

[8] L. Navarro, et al., Thermal energy storage in building integrated thermal systems: a review. Part 2. Integration as passive system, Renew. Eng. 85 (2016) 1334-1356.

[9] G. Lydon, et al., Coupling energy systems with lightweight structures for a net plus energy building, Appl. Eng. 189 (2017) 310-326.

[10] P. Hoes, et al., Investigating the potential of a novel low-energy house concept with hybrid adaptable thermal storage, Eng. Convers. Manag. 52 (6) (2011) 2442-2447.

[11] P. Hoes, J. Hensen, The potential of lightweight low-energy houses with hybrid adaptable thermal storage: comparing the performance of promising concepts, Eng. Build. 110 (2016) 79-93.

[12] J. Gelegenis, P. Axaopoulos, A multi-parametric mathematical approach on the selection of optimum insulation thicknesses in buildings, Buildings 7 (1) (2017) 15.

[13] H.U. Rehman, Experimental performance evaluation of solid concrete and dry insulation materials for passive buildings in hot and humid climatic conditions, Appl. Eng. 185 (2017) 1585-1594.

[14] P. Hoes, et al., Exploring the Optimal Thermal Mass to Investigate the Potential of a Novel Low-energy House Concept, 2010.

[15] M. Ren, J. Wright, A ventilated slab thermal storage system model, Build. Environ. 33 (1) (1998) 43-52.

[16] D. Zhou, C.-Y. Zhao, Y. Tian, Review on thermal energy storage with phase change materials (PCMs) in building applications, Appl. Eng. 92 (2012) 593-605.

[17] M.S.-E. Imbabi, E. Elsarrag, T.G. O'hara, Dynamic Insulation Systems, Google Patents, 2012.

[18] F. Roberz, et al., Ultra-lightweight concrete: energy and comfort performance evaluation in relation to buildings with low and high thermal mass, Eng. Build. 138 (2017) 432-442.

[19] P. Devi, S. Palaniappan, A case study on life cycle energy use of residential building in Southern India, Eng. Build. 80 (2014) 247-259.

[20] S.S. Shrestha, A.O. Desjarlais, J.A. Atchley, Thermal Performance Evaluation of Walls with Gas Filled Panel Insulation, Oak Ridge National Lab.(ORNL), Oak Ridge, TN (United States), 2014. Building Technologies Research and Integration Center (BTRIC).

[21] D.B. Crawley, et al., Contrasting the capabilities of building energy performance simulation programs, Build. Environ. 43 (4) (2008) 661-673.

[22] H.S. Rallapalli, A Comparison of EnergyPlus and EQUEST Whole Building Energy Simulation Results for a Medium Sized Office Building, Arizona State University, 2010.

[23] A. Yezioro, B. Dong, F. Leite, An applied artificial intelligence approach towards assessing building performance simulation tools, Eng. Build. 40 (4) (2008) 612-620.

[24] W.A. Friess, K. Rakhshan, A review of passive envelope measures for improved building energy efficiency in the UAE, Renew. Sustain. Eng. Rev. 72 (2017) 485-496.

[25] O. Siddiqui, et al., Modelling for performance prediction of highly insulated buildings with different types of thermal mass, Appl. Therm. Eng. 122 (2017) 139-147.

[26] S.A. Al-Sanea, M. Zedan, S.A. Al-Ajlan, Effect of electricity tariff on the optimum insulation-thickness in building walls as determined by a dynamic heat-transfer model, Appl. Eng. 82 (4) (2005) 313-330.

[27] O. Kaynakli, Parametric investigation of optimum thermal insulation thickness for external walls, Energies 4 (6) (2011) 913-927.

[28] L. Aditya, et al., A review on insulation materials for energy conservation in buildings, Renew. Sustain. Eng. Rev. 73 (2017) 1352-1365.

[29] J. Kosny, et al., Thermal Mass-energy Savings Potential in Residential Buildings, Report no., Buildings Technology Center, ORNL, 2001.

[30] S. Naji, et al., Structure, energy and cost efficiency evaluation of three different lightweight construction systems used in low-rise residential buildings, Eng. Build. 84 (2014) 727-739.

[31] Y. Wang, Optimization for Building Control Systems of a School Building in Passive House Standard, Universität München, 2015.

[32] A.K. Athienitis, M. Santamouris, Thermal Analysis and Design of Passive Solar Buildings, Routledge, 2013.

[33] S.A. Al-Sanea, M. Zedan, S. Al-Hussain, Effect of thermal mass on performance of insulated building walls and the concept of energy savings potential, Appl. Eng. 89 (1) (2012) 430-442.

[34] W. Liping, W.N. Hien, The impacts of ventilation strategies and facade on indoor thermal environment for naturally ventilated residential buildings in Singapore, Build. Environ. 42 (12) (2007) 4006-4015.

[35] K.S. Al-Jabri, et al., Concrete blocks for thermal insulation in hot climate, Cement Concr. Res. 35 (8) (2005) 1472-1479.

[36] U.J. Alengaram, et al., A comparison of the thermal conductivity of oil palm shell foamed concrete with conventional materials, Mater. Des. 51 (2013) 522-529.

[37] S.-C. Ng, K.-S. Low, Thermal conductivity of newspaper sandwiched aerated lightweight concrete panel, Eng. Build. 42 (12) (2010) 2452-2456.

[38] A.T. Almalkawi, S. Hamadna, P. Soroushian, One-part alkali activated cement based volcanic pumice, Construct. Build. Mater. 152 (2017) 367-374.

[39] A.T. Almalkawi, W. Hong, S. Hamadna, P. Soroushian, G. Al-Chaar, Behavior of a lightweight frame made with aerated slurry-infiltrated chicken mesh under cyclic lateral loading, Construct. Build. Mater. 160 (2018) 679-686.

[40] A.T. Almalkawi, T. Salem, S. Hamadna, A.G.N.D. Darsanasiri, P. Soroushian, A. Balchandra, G. Al-Chaar, Physio-microstructural properties of aerated cement slurry for lightweight structures, Materials 11 (4) (2018) 597.

[41] A.T. Almalkawi, W. Hong, S. Hamadna, P. Soroushian, A.G.N.D. Darsanasiri, A. Balchandra, G. Al-Chaar, Mechanical properties of aerated cement slurry-infiltrated chicken mesh, Construct. Build. Mater. 166 (2018) 966-973.

[42] W. Wu, F. Matalkah, P. Soroushian, A. Almalkawi, X. Wang, L. Xu, Influence of admixtures on rheological properties and heat of hydration of alkali aluminosilicate cement, Adv. Cem. Res. 29 (9) (2017) 397-403.

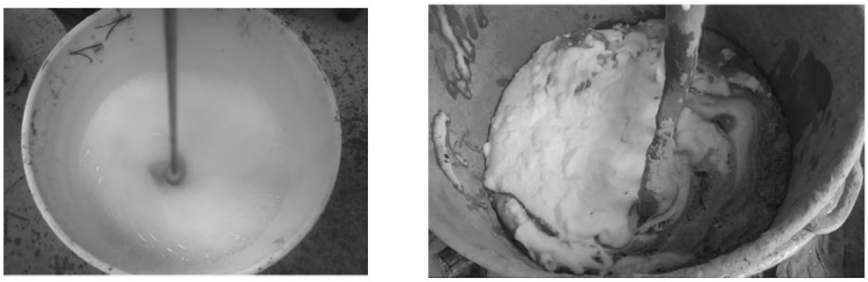

(a) Mixing of the foaming agent with water (b) Mixing of foamed water with dement

Figure 1. Preparation of the aerated slurry.

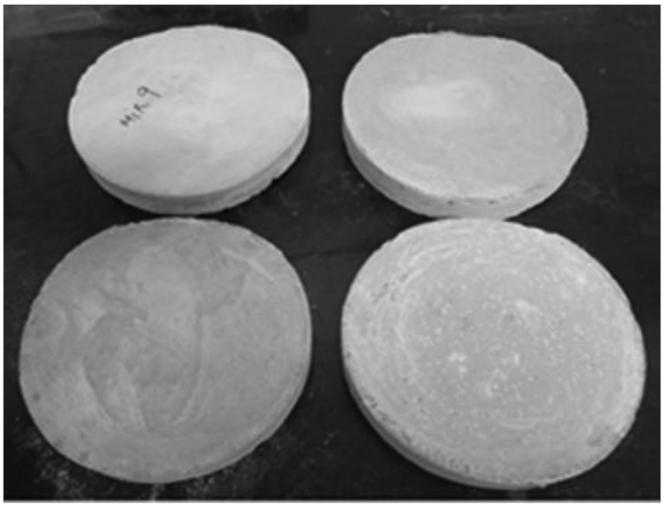

Figure 2. Examples of the aerated slurry thermal conductivity test specimens.

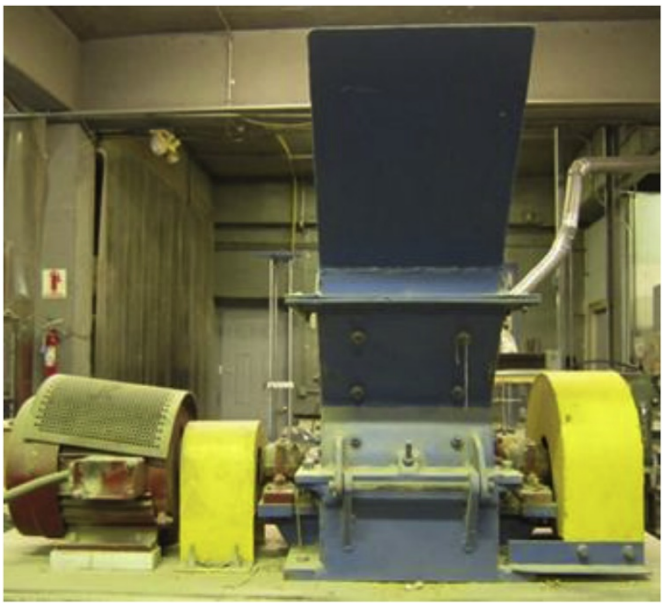

Figure 3. The hammer mill used for shredding of straw.

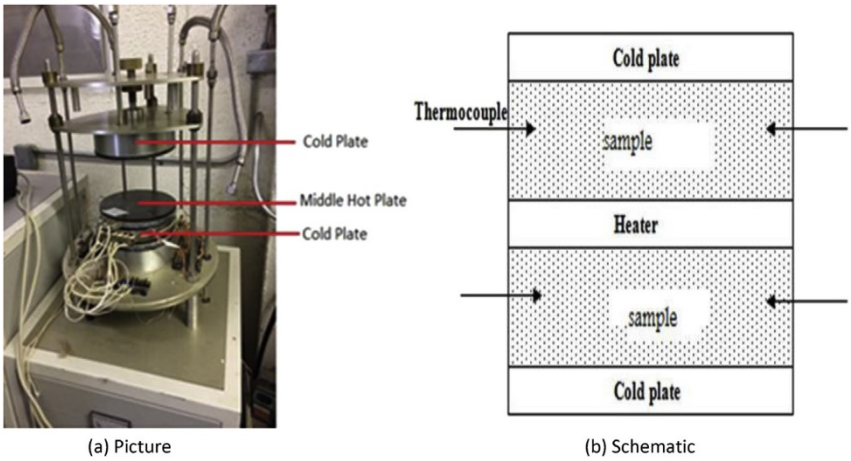

Figure 4. Thermal conductivity test setup.

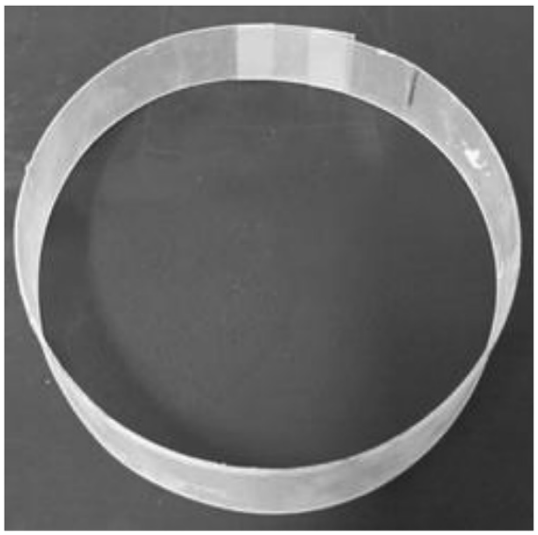

Figure 5. The polypropylene ring used to prepare biomass insulation materials.

Figure 6. Thermal conductivity test specimens for different biomass insulation materials.

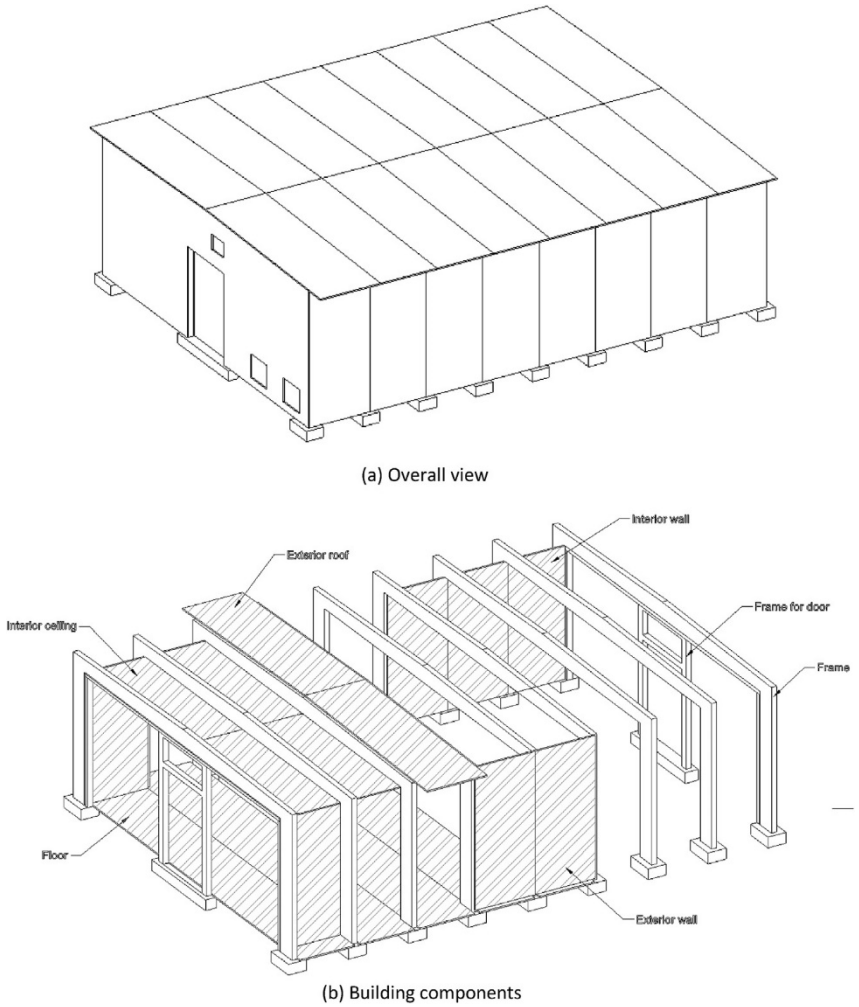

Figure 7. The building system.

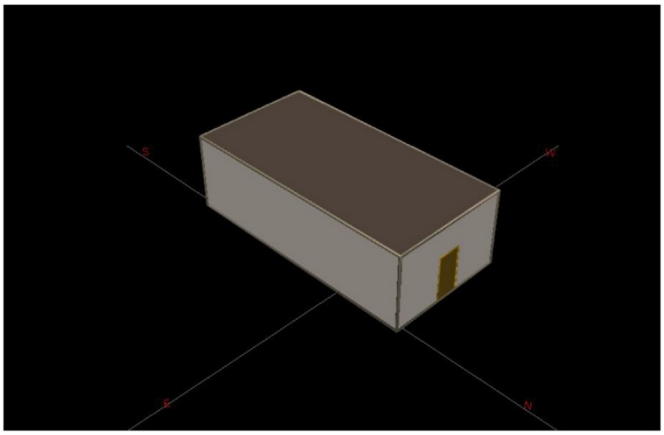

Figure 8. The building orientation.

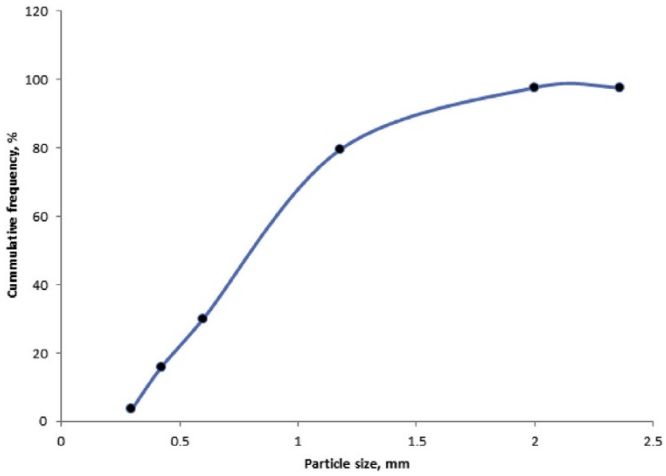

Figure 9. Particle size distribution of the ground wood insulation.

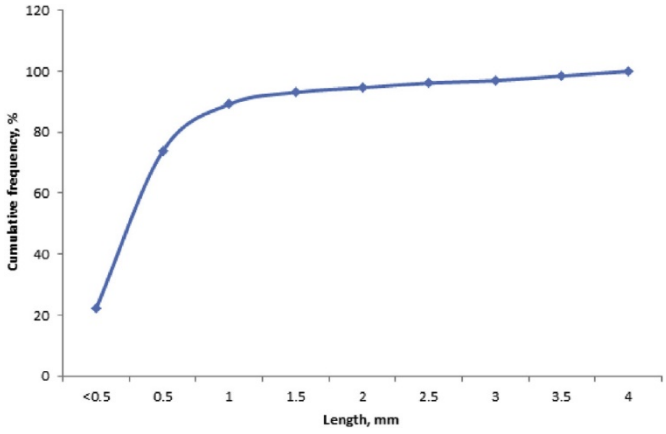

Figure 10. Length distribution of the shredded straw.

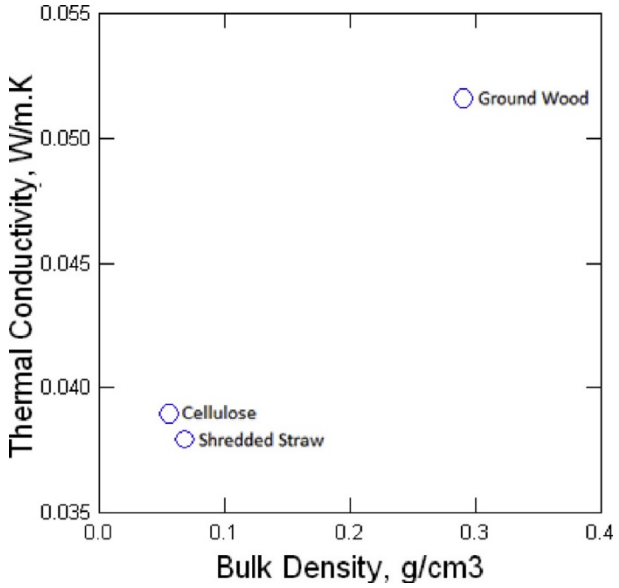

Figure 11. The relationship between the thermal conductivity and the bulk density of the three biomass-based loose insulation materials.

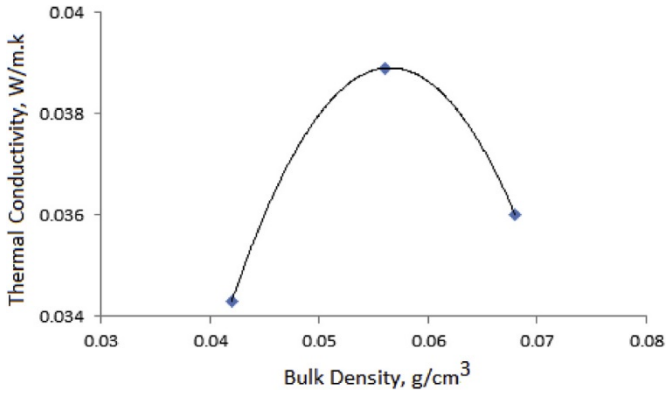

Figure 12. Effect of the cellulose insulation bulk density on its thermal conductivity.

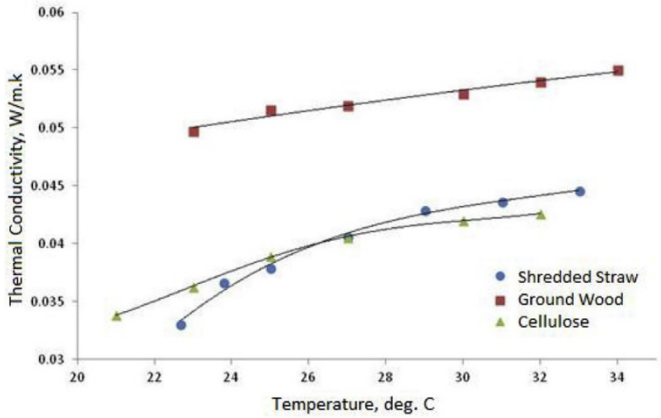

Figure 13. Thermal conductivity versus temperature for the loose biomass-based insulation materials.

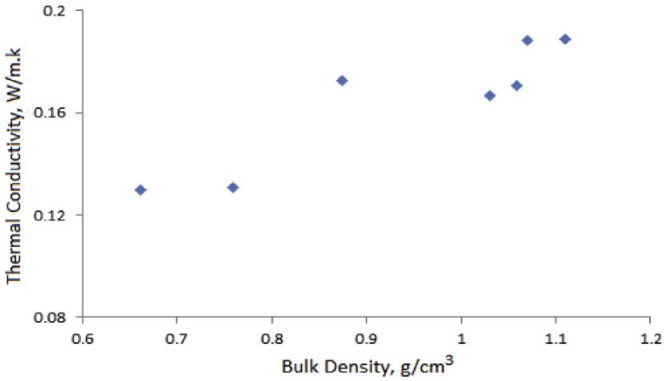

Figure 14. Thermal conductivity test results for aerated slurries of different bulk densities.

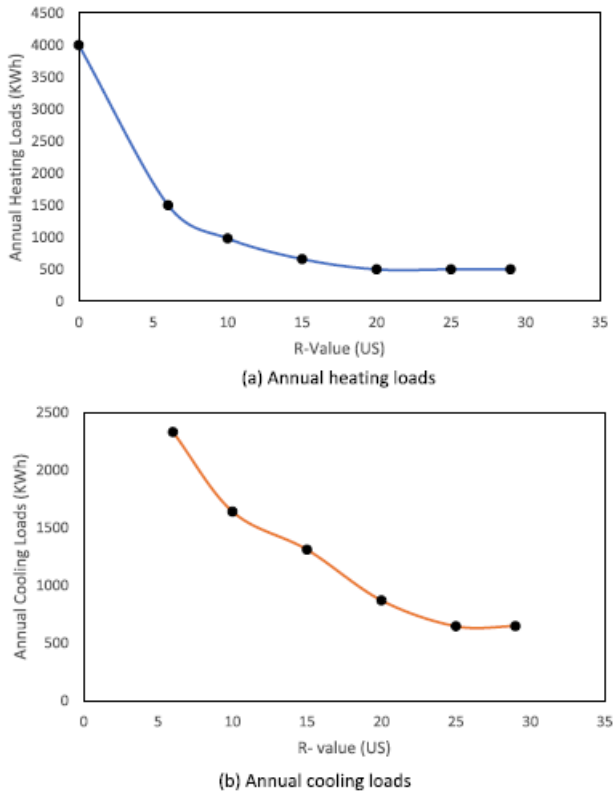

Figure 15. Effects of the wall insulation on the cooling and heating loads of the building (RSI (K.m^2/W) = R-value (US) (ft^2. °F.hr/Btu)/5.68).

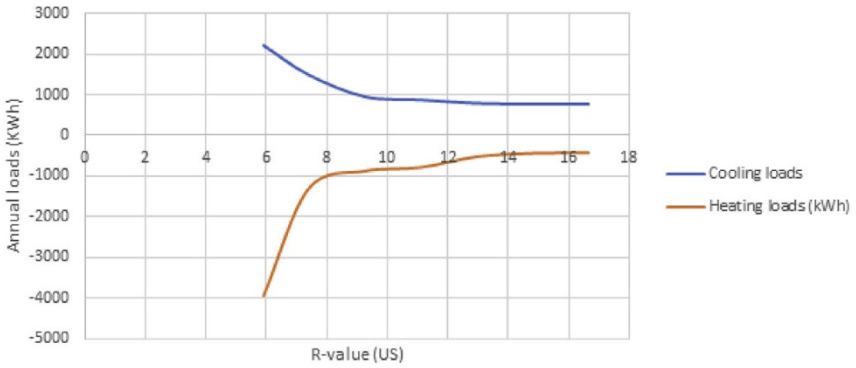

Figure 16. Effects of the roof insulation on the cooling and heating loads of the building (RSI (K.m^2/W) = R-value (US) (ft^2. °F.hr/Btu)/5.68).

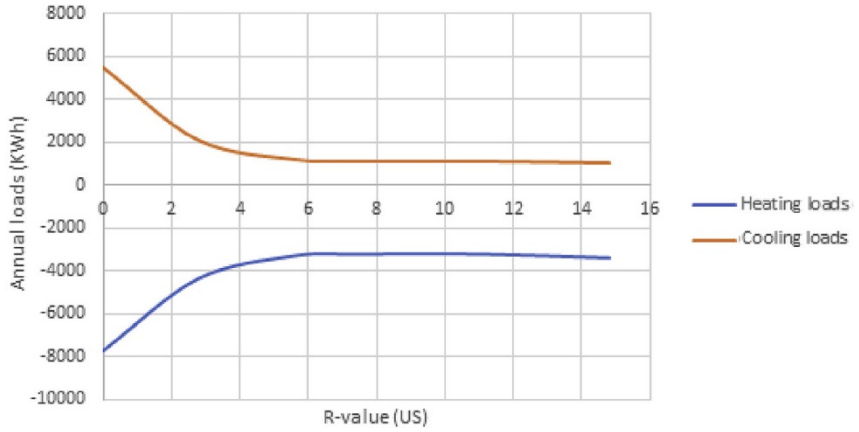

Figure 17. Effects of the roof insulation on the cooling and heating loads of the building (RSI (K.m^2/W) = R-value (US) (ft^2. °F.hr/Btu)/5.68).

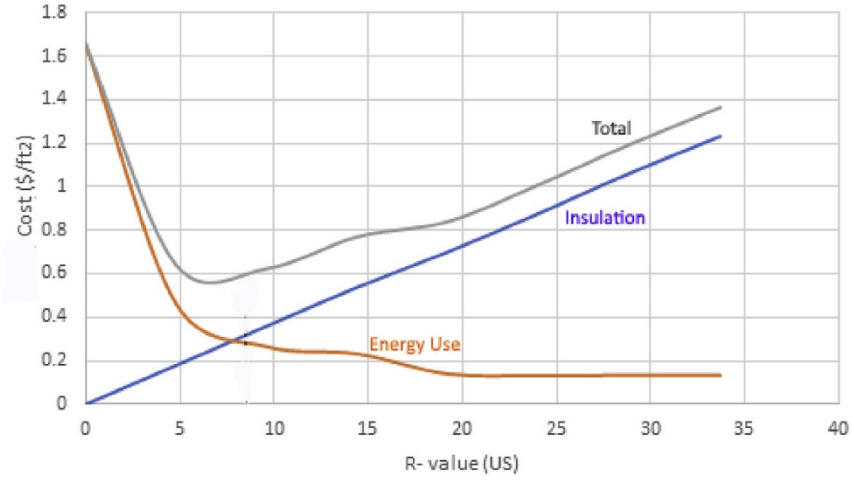

Figure 18. The heating/cooling, insulation and total costs versus the wall insulation condition.

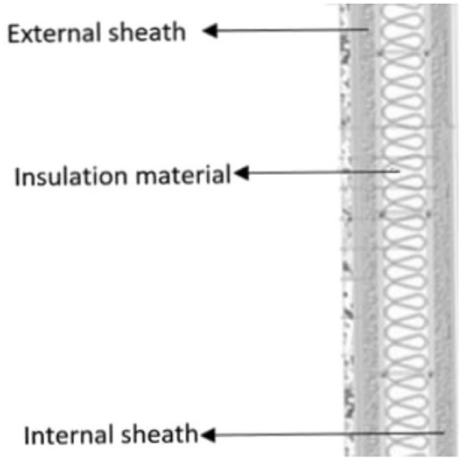

Figure 19. Schematics of a layered wall structure.

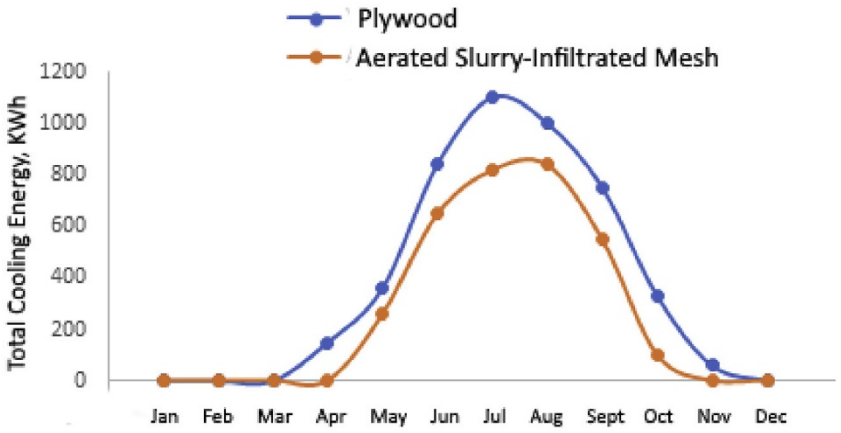

Figure 20. Cooling energy demand of the two building systems.

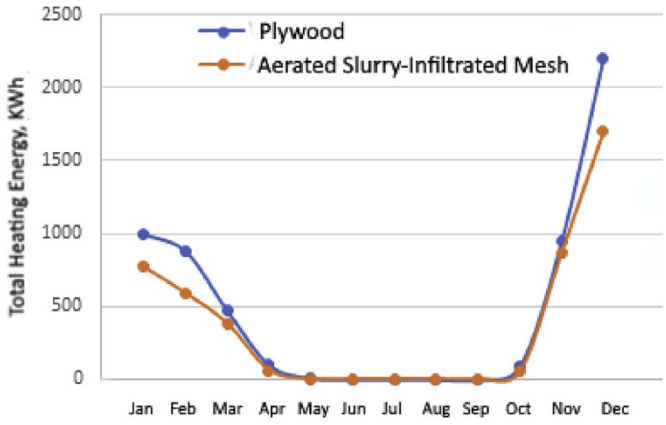

Figure 21. Heating energy demands of the two building systems.